

# *Analytical Models of Effective DOS, Saturation Velocity and High-Field Mobility for SiGe HBTs Numerical Simulation*

G. Sasso, N. Rinaldi

Department of Biomedical, Electronics and  
Telecommunications Engineering,  
University of Naples “Federico II”  
via Claudio 21, 80125 Naples, Italy  
grazia.sasso@unina.it

G. Matz, C. Jungemann

Institute for Microelectronics and Circuits,  
Bundeswehr University  
85577 Neubiberg, Germany

**Abstract**—Effective density of state, saturation velocity and high field mobility analytical models for hydrodynamic simulation of silicon-germanium hetero-junction bipolar transistors have been derived.

**TCAD; Device Simulation; SiGe HBTs; Effective DOS; Saturation Velocity; High-Field Mobility.**

## 1. INTRODUCTION

As demonstrated by recent published results [1], the aggressive technology development effort of the DOTFIVE project [2] has been significantly advancing the performance of SiGe:C heterojunction bipolar transistors (HBTs) towards the Terahertz range. Performance improvement needs to be supported by reliable Technology Computer Aided Design (TCAD) tools. However, realistic and predictive simulation results require suitable models for all involved physical parameters. Here we propose new calibrated analytical models for effective densities of states (DOS), carrier saturation velocity and high-field mobility for energy transport/hydrodynamic (ET/HD) simulations; the present work improves models available in literature, including the dependence on all relevant parameters. Models calibration has been performed by means of an experimentally verified full-band MC simulation code [3]. The new proposed models have been implemented in a commercial tool [4]; however, implementation results are omitted here for brevity. The present work complements the results in [5], hence providing a complete analytical model set for realistic and predictive SiGe HBTs device simulation.

## 2. EFFECTIVE DENSITY OF STATES MODELS

SiGe device simulation requires a suitable model for effective Densities of States (DOS), due to their outstanding role in collector current computation. A simplified approximation was proposed in [6], lying in a constant ratio between the product of the effective DOS for silicon-germanium and silicon according to (1).

$$(N_c N_v)_{\text{SiGe}} / (N_c N_v)_{\text{Si}} \approx 0.4 \quad (1)$$

The constant ratio approximation disregards some critical dependences, which fill a key role for effective DOS evaluation. In SiGe the bands degeneracies split due to

strain, and effective DOS are consequently modified. For low Ge content the split is of the order of  $k_B T_L$  [7], so that a strong dependence on lattice temperature ( $T_L$ ) is expected. Whereas this effect cannot be neglected, dependences on the mole fraction ( $x$ ) and lattice temperature must be taken into account in effective DOS models.

Effective densities are typically proposed in device simulators as functions of effective masses, [4]; however, analytical formulation including dependence on effective mass is based upon the assumption of scalar effective mass. In order to ride over this limitation and provide a general effective DOS model, able to be implemented in different device simulators using their characteristic relation tying the effective DOS to the effective mass, we formulate SiGe effective densities as functions of the silicon ones. Besides, silicon effective DOS dependence on lattice temperature is developed starting from the well-known power law dependence [8] and optimizing the exponents in (2) and (3) using MC data.

$$N_c(T_L) = N_{c\_300} \cdot (T_L/T_0)^{a_c}, \quad T_0 = 300 \text{ K} \quad (2)$$

$$N_v(T_L) = N_{v\_300} \cdot (T_L/T_0)^{a_v}, \quad T_0 = 300 \text{ K} \quad (3)$$

The model for SiGe conduction band proposed in [9] includes main dependences, computing effective DOS for electrons as in (4), where the parameters can be extracted from the schematic view of band degeneracy splitting proposed by Prinz [7]:

$$N_{c,\text{Si}_{1-x}\text{Ge}_x}(T_L, x) = N_{c,\text{Si}}(T_L) \cdot \frac{M_{c1} + M_{c2} \cdot \exp\left(\frac{\Delta E_c \cdot x}{k_B \cdot T_L}\right)}{M_{c1} + M_{c2}} \quad (4)$$

On the other hand, SiGe valence band effective DOS is usually fixed as in bulk silicon [9] or assumed to be linearly dependent on the mole fraction [10]. We propose an analytical approximation for the hole effective DOS which includes the Ge mole fraction and lattice temperature dependences. A new model has been developed starting from the splitting schematic view in [7], providing the sum between  $\Delta E_{v1}$  and  $\Delta E_{v2}$  as 0.125 eV for 20% germanium mole fraction; single terms of the sum have been arranged to fit (5) with MC data.

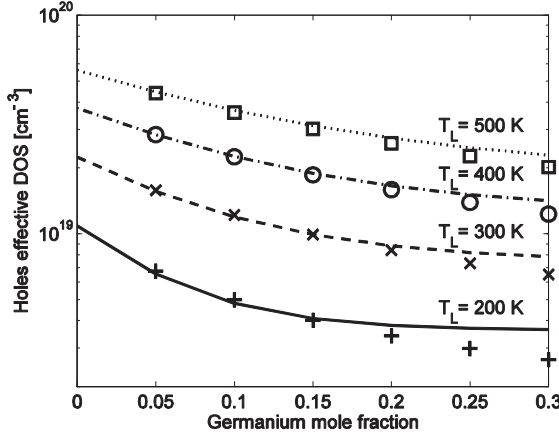


Figure 1.  $\text{Si}_{1-x}\text{Ge}_x$  valence band effective DOS as a function of Ge mole fraction for several lattice temperatures. Lines: model; symbols: MC data.

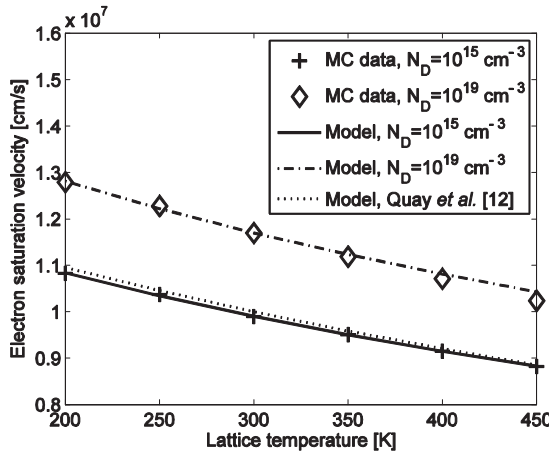


Figure 2. Electron saturation velocity in silicon as a function of lattice temperature for several doping concentrations. Model [12] provides a reasonable fit only for low doping levels.

$$N_{V_{\text{Si}_{1-x}\text{Ge}_x}}(T_L, x) = N_{V_{\text{Si}}}(T_L) \cdot \frac{M_{V1} + M_{V2} \cdot \exp\left(\frac{\Delta E_{V1} \cdot x}{k_B \cdot T_L}\right) + M_{V3} \cdot \exp\left(\frac{\Delta E_{V2} \cdot x}{k_B \cdot T_L}\right)}{M_{V1} + M_{V2} + M_{V3} \cdot \exp\left(\frac{\Delta E_{V3}}{k_B \cdot T_L}\right)} \quad (5)$$

The effective DOS model results for holes are depicted in Fig. 1 and model parameters are summarized in TABLE I. The new model provides an accurate approximation for valence band effective DOS in the mole fraction range stocked in the base region of SiGe HBTs ( $0 \div 0.2$ ).

TABLE I. PARAMETERS FOR SiGE ALLOY EFFECTIVE DOS

Parameter	Value	Parameter	Value
$N_{C_{300}} [\text{cm}^{-3}]$	$2.94 \cdot 10^{19}$	$N_{V_{300}} [\text{cm}^{-3}]$	$2.24 \cdot 10^{19}$
$\alpha_C$	1.62	$\alpha_V$	1.79
$M_{C1}$	4	$M_{V1}=M_{V2}=M_{V3}$	1
$M_{C2}$	2	$\Delta E_{V1} [\text{eV}]$	-0.31
$\Delta E_C [\text{eV}]$	-0.6	$\Delta E_{V2} [\text{eV}]$	-0.315
		$\Delta E_{V3} [\text{eV}]$	-0.044

### 3. CARRIER SATURATION VELOCITY MODEL

Saturation velocity generally appears in high-field mobility models; therefore an accurate model embodying all relevant dependences is mandatory. In [11] Ershov *et al.* propose a simple model including the dependence on Ge mole fraction and the model in [12] adds the lattice temperature influence. However, all available models neglect dependence upon doping level. By MC investigation we verified that saturation velocity can vary with doping level more than 10% (Fig. 2). Thus, a new model has been developed which includes the dependence upon lattice temperature, Ge mole fraction and doping ( $N$ ). The new model for bulk silicon is given by (6) and (7), where  $N_{\text{REF}}$  is fixed to  $10^{16} \text{ cm}^{-3}$ .

$$v(N, T_L) = \frac{v_{300}(N)}{1 - A \cdot (1 - (T_L/T_0)^b)} \quad (6)$$

$$v_{300}(N) = v_1 \cdot (N/N_{\text{REF}})^g \quad (7)$$

Model extension to include dependence upon Ge mole fraction is given by

$$v_{\text{SiGe}} = v_{\text{Si}} \cdot (1 - x_n) + v_{\text{Si}_{0.7}\text{Ge}_{0.3}} \cdot x_n + (1 - x_n^a) \cdot x_n^a \cdot C_v \quad (8)$$

where  $C_v$  is a bowing factor

The germanium content  $x_n$  is normalized to 0.3, since in SiGe HBTs the germanium mole fraction never exceeds 0.3 (typically the maximum value is about 0.2). Limiting the mole fraction calibration range improves model accuracy. Model parameters are summarized in TABLE II for both electrons and holes, results and comparison with MC data are depicted in Fig. 2 and Fig. 3.

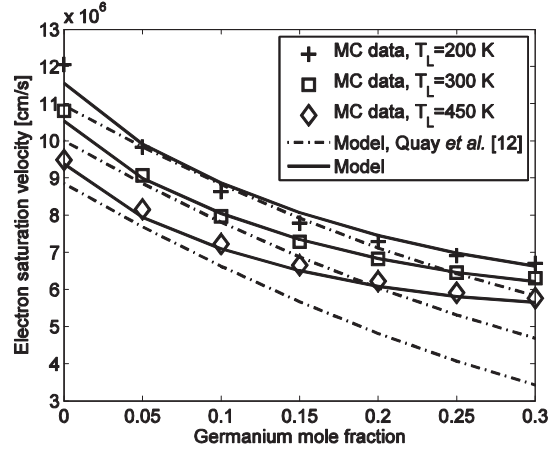


Figure 3. Electron saturation velocity in  $\text{Si}_{1-x}\text{Ge}_x$  as a function of Ge mole fraction for several lattice temperatures.  $N=N_D=10^{18} \text{ cm}^{-3}$ .

TABLE II. SATURATION VELOCITY MODEL PARAMETERS.

Parameter	Electrons		Holes
	$\text{Si} (x_n=0)$	$\text{Si}_{0.7}\text{Ge}_{0.3} (x_n=1)$	
$v_1 [\text{cm/s}]$	$9.954 \cdot 10^6$	$1.1412 \cdot 10^7$	
$g$	0.0127	0.0084	
$A$	0.3163	0.218	
$b$	0.8091	1.0693	
$\text{Si}_{0.7}\text{Ge}_{0.3} (x_n=1)$	$\text{Si} (x_n=0)$		
	$v_1 [\text{cm/s}]$	$6.093 \cdot 10^6$	$8.1459 \cdot 10^6$
	$g$	0.004	0.0062
	$A$	0.175	0.1284
$b$	1.1048	1.24	
$C_v [\text{cm/s}]$	$-5.262 \cdot 10^6$	$-2.22 \cdot 10^6$	
$\alpha$	0.74665	0.8223	

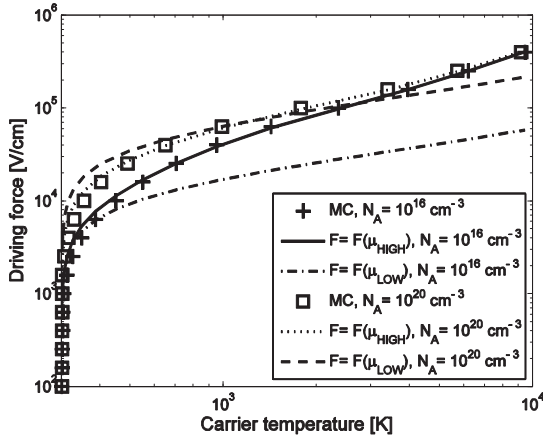


Figure 4. Electric field in homogeneous silicon (MC data) and effective driving force computed by using  $\mu_{\text{HIGH}}$  and  $\mu_{\text{LOW}}$  MC data in (9).

#### 4. HIGH-FIELD MOBILITY MODEL

With the ongoing downscaling of devices, the use of ET and HD models has become mandatory, in order to capture nonlocal effects in modern miniaturized devices. It is well known that in the presence of a strong electric field electrons gain energy and their temperature is highly increased [13]. The carrier temperature gradient introduces an additional driving force and in TCAD HD simulations the electric field is replaced by an effective driving force, [4] and [14]. Effective driving force is derivable from the homogeneous steady state energy balance equation, resulting in (9), where  $\tau_E$  is the carrier energy relaxation time,  $W_0$  and  $W_C$  are lattice and carriers (electrons/holes) energies and are given by (10):

$$F = \sqrt{\max(W_C - W_0, 0) / (\tau_E \cdot q \cdot \mu_{\text{HIGH}})} \quad (9)$$

$$W_0 = 3 \cdot k_B \cdot T_L / 2, \quad W_C = 3 \cdot k_B \cdot T_C / 2 \quad (10)$$

Several high-field mobility models for HD simulation include a direct dependence upon the carrier temperature, [15] and [16]. However, these models are derived by substituting the high-field mobility  $\mu_{\text{HIGH}}$  in (9) with the low-field one  $\mu_{\text{LOW}}$ , hence, losing consistency between electric field and the effective driving force in the homogenous case, as verified applying (9) on MC data, Fig. 4. Low field mobility and energy relaxation time are computed using models in [5].

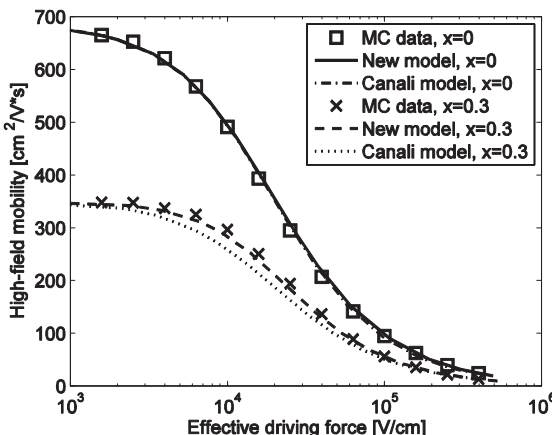


Figure 5. High field mobility as a function of effective driving force given in (9).  $T_L = 300 \text{ K}$ ,  $N = N_A = 10^{18} \text{ cm}^{-3}$ .

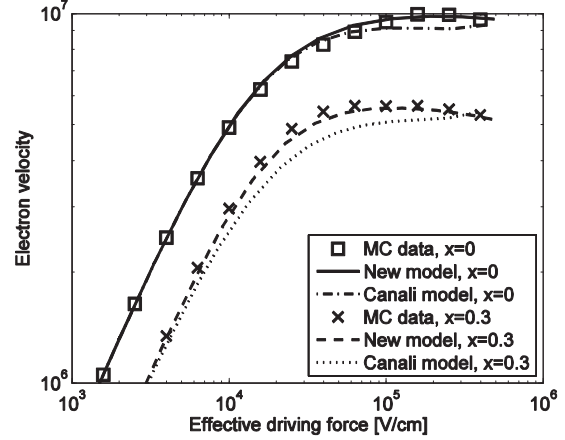


Figure 6. Electron velocity as function of effective driving force computed by using (9). Velocity is calculated as the product between mobility and driving force.  $T_L = 300 \text{ K}$ ,  $N = N_A = 10^{18} \text{ cm}^{-3}$ .

A more general approach is available in commercial device simulators [4], combining the effective driving force (9) with the well known empirical model by Canali *et al.* [17], (11).

$$\mu_{\text{HIGH}} = \mu_{\text{LOW}} \left[ 1 + ((F \cdot \mu_{\text{LOW}}) / v_{\text{sat}})^{\beta} \right]^{1/\beta} \quad (11)$$

However this formulation has been verified to be not suitable for SiGe, since it doesn't provide an accurate dependence on all relevant variables (see Fig. 5); moreover, it does not account for the negative differential electron drift velocity (Gunn effect) as shown in Fig. 6. The extended Canali model is based on the saturation assumption for carrier velocity, therefore resulting carrier velocity, given by the product between carrier mobility and effective driving force, cannot describe the actual behavior. Although the Gunn effect is well known for III-IV semiconductors, it has been verified that the transition of electrons from the twofold valley to the fourfold valley can occur in SiGe as well [18],[19], but no analytical mobility model has ever looked on it. Thus, we propose a new analytical high-field mobility model, using (9) as driving force and providing an accurate predictive function of mobility values with lattice temperature, carrier temperature, doping values and mole fraction. The complete model is reported in (12)÷(15) and in TABLE III ( $N_{\text{REF}}$  in (13) is fixed to  $10^{15} \text{ cm}^{-3}$ ):

$$\mu_{\text{HIGH}} = \mu_{\text{LOW}} \left\{ \left[ 1 + (F/F_R)^{\alpha} \right] \cdot \left[ 1 + ((F \cdot \mu_{\text{LOW}}) / v_{\text{sat}})^{\beta} \right]^{1/\beta} \right\} \quad (12)$$

$$\beta = \beta_0 + \beta_1 \cdot \log_{10}(1+x_n) + (\beta_2 \cdot \log_{10}(N/N_{\text{REF}}))^{\beta_3} \quad (13)$$

$$\alpha = \alpha_0 - \alpha_1 \cdot \log_{10}(1+x_n) \quad (14)$$

$$F_R = \frac{T_0}{T_L} \cdot \exp(F_{R0} - F_{R1} \cdot \log_{10}(N/N_{\text{REF}})) \quad (15)$$

The new formulation consists of a nonlinear equations system ((9) and (12)÷(15)), whose unknown quantities are  $F$  and  $\mu_{\text{HIGH}}$ ; its numerical solution provides the effective driving force results depicted in Fig. 7, which are in good agreement with MC data. The new model includes the dependences on carrier temperature, lattice temperature and mole fraction (Fig. 8 and Fig. 9). The accuracy is strongly improved compared to the extended Canali model (Fig. 5 and Fig. 6). Additionally, it predicts the negative differential slope of electron velocity versus electric field (Fig. 9). Since holes have no “hot effects”, the model (11), combined with (13), can still be used for holes.

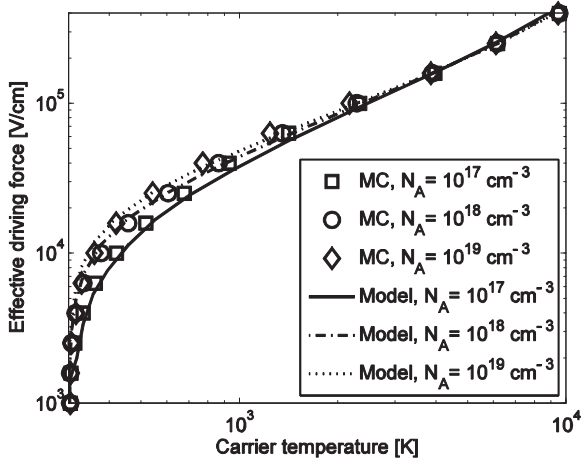


Figure 7. Effective driving force in silicon for minority electrons as a function of electron temperature for several doping concentrations.  $T_L=300$  K.

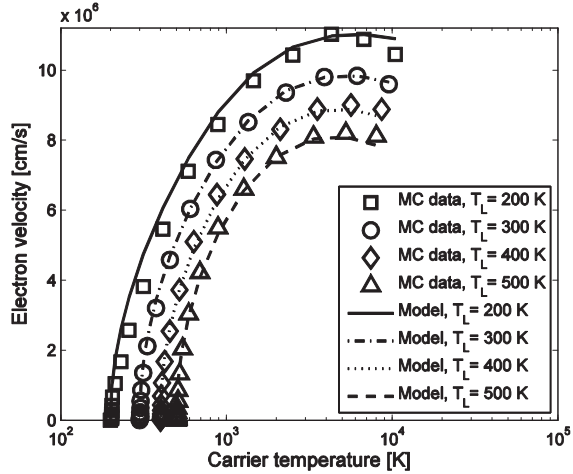


Figure 8. Electron drift velocity in silicon ( $\mu_{\text{HIGH-F}}$ ) as a function of electron temperature for several lattice temperatures;  $N=N_A=10^{18} \text{ cm}^{-3}$ .

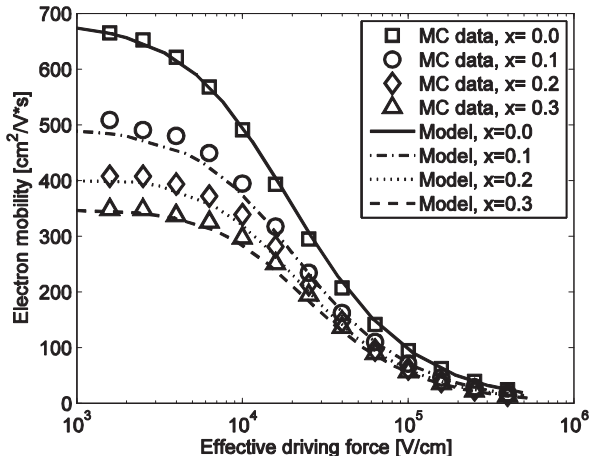


Figure 9. Out-of-plane minority electron mobility in  $\text{Si}_{1-x}\text{Ge}_x$  as a function of effective driving force for several germanium mole fraction;  $N=N_A=10^{17} \text{ cm}^{-3}$ ,  $T_L=300$  K.

#### ACKNOWLEDGMENT

The authors would like to thank the support of the European Commission in the frame of the FP7 IST project DOTFIVE (IST-216110).

TABLE III. HIGH-FIELD MOBILITY MODEL PARAMETERS

Parameter	Electrons	Holes
$\beta_0$	1.26	1.1
$\beta_1$	1	0
$\beta_2$	0.07	0.09
$\beta_3$	1	2
$\alpha_0$	1	-
$\alpha_1$	1.4	-
$F_{R0}$	-16.8112	-
$F_{R1}$	0.3979	-

#### REFERENCES

- [1] P. Chevalier, F. Pourchon, T. Lacave, G. Avenier, Y. Campidelli, L. Depoyan, G. Troillard, M. Buczko, D. Gloria, D. Céli, C. Gaquière, and A. Chantre, "A conventional double-polysilicon FSA-SEG Si/SiGe:C HBT reaching 400 GHz fmax," Proc. BCTM, pp. 1-4, October 2009
- [2] <http://www.dotfive.eu/>
- [3] C. Jungemann, S. Keith, and B. Meinerzhagen, "Full-band Monte Carlo device simulation of a Si/SiGe-HBT with a realistic Ge profile," IEICE Trans. Electron., vol. E83-C, no. 8, pp. 1228-1234, 2000.
- [4] Synopsys TCAD Software, Release 2007.03.
- [5] G. Sasso, G. Matz, C. Jungemann, and N. Rinaldi, "Accurate mobility and energy relaxation time models for SiGe HBTs numerical simulation," Proc. SISPAD, pp. 241-244, September 2009.
- [6] R. J. E. Huetting, J. W. Slotboom, A. Pruijboom, W. B. de Boer, C. E. Timmering, and N. E. B. Cowern, "On the optimization of SiGe-base bipolar transistors," IEEE Trans. on Elect. Devices, vol. 43, no. 9, pp. 1518-1524, 1996.
- [7] E. J. Prinz, P. M. Garone, P. V. Schwartz, X. Xiao, and J. C. Sturm, "The effect of base-emitter spacers and strain-dependent densities of states in Si/Si<sub>1-x</sub>Ge<sub>x</sub>/Si heterojunction bipolar transistors," Proc. IEDM, pp. 639-642, December 1989.
- [8] M. A Green, "Intrinsic concentration, effective densities of states, and effective mass in silicon," J. Appl. Phys. 1990, vol. 67, no. 6, pp. 2944-2954.
- [9] B. Pejcincovic, L. E. Kay, T. Tang, and D. H. Navon, "Numerical simulation and comparison of Si BJT's and Si<sub>1-x</sub>Ge<sub>x</sub> HBT's," IEEE Trans. on Elect. Devices, vol. 36, no. 10, pp. 2129-2137, 1989.
- [10] R. People, "Physics and applications of Ge<sub>x</sub>Si<sub>1-x</sub>/Si strained-layer heterostructures," IEEE Jurnal of Quantum Electronics, Vol. QE-22, No. 9, 1986.
- [11] M. Ershov, and V. Ryzhii, "High-field electron transport in SiGe alloy," Jpn. J. Appl. Phys., vol 33, p. 1365-1371, 1994.
- [12] R. Quay, C. Moglestone, V. Palankovski, and S. Selberherr, "A temperature dependent model for the saturation velocity in semiconductor materials," Mat. Sci. Semic. Proc. vol. 3, pp. 149-155, 2000;
- [13] T. Grasser, T.-W. Tang, H. Kosina, and S. Selberherr, "A review of hydrodynamic and energy-transport models for semiconductor device simulation," Proc. IEEE, vol. 91, no. 2, pp. 251-274, 2003.
- [14] Atlas Users Manual, SILVACO, 2000.
- [15] V. Palankovski, and R. Quay, Analysis and Simulation of Heterostructure Devices. Wien: Springer, 2004.
- [16] Y. Apanovich, E. Lyumkis, B. Polksy, A. Shur, and P. Blakey, "Steady-state and transient analysis of submicron devices using energy balance and simplified hydrodynamic models," IEEE Trans. on CAD, vol. 13, no. 6, pp. 702-711, 1994.
- [17] C. Canali, C. Jacoboni, F. Nava, G. Ottaviani, and A. Alberighi-Quaranta, "Electron drift velocity in silicon," Phys. Rev. B, vol. 12, no. 4, pp. 2265-2284, 1975
- [18] B. K. Ridley, and T. B. Watkins, "The possibility of negative resistance effects in semiconductors," Proc. Phys. Soc., vol. 78 n. 2, pp. 293-304, 1961.
- [19] F. M. Busler, P. Graf, S. Keith, and B. Meinerzhagen, "Full band Monte Carlo investigation of electron transport in strained Si grown on Si<sub>1-x</sub>Ge<sub>x</sub> substrates," Appl. Phys. Lett., vol. 70 no. 16, pp. 2144-2146, 1997.